Rapid Communications

Random singlet state in $Ba_5CuIr_3O_{12}$ single crystals

Pavel A. Volkov,[1,2,*] Choong-Jae Won,[3,4] D. I. Gorbunov,[5] Jaewook Kim,[1,6] Mai Ye,[1,†] Heung-Sik Kim,[1,7] J. H. Pixley,[1,2] Sang-Wook Cheong,[1,3,4,6] and G. Blumberg[1,8,‡]

[1]*Department of Physics and Astronomy, Rutgers University, Piscataway, New Jersey 08854, USA*
[2]*Center for Materials Theory, Rutgers University, Piscataway, New Jersey 08854, USA*
[3]*Max Planck POSTECH/Korea Research Initiative, Pohang University of Science and Technology, Pohang 37673, Korea*
[4]*Laboratory of Pohang Emergent Materials, Pohang Accelerator Laboratory, Pohang 37673, Korea*
[5]*Hochfeld-Magnetlabor Dresden (HLD-EMFL), Helmholtz-Zentrum Dresden-Rossendorf, 01328 Dresden, Germany*
[6]*Rutgers Center for Emergent Materials, Rutgers University, Piscataway, New Jersey 08854, USA*
[7]*Department of Physics, Kangwon National University, Chuncheon 24341, Korea*
[8]*National Institute of Chemical Physics and Biophysics, 12618 Tallinn, Estonia*

(Received 1 August 2019; revised manuscript received 31 October 2019; published 15 January 2020)

We study the thermodynamic and high-magnetic-field properties of the magnetic insulator $Ba_5CuIr_3O_{12}$, which shows no magnetic order down to 2 K, consistent with a spin-liquid ground state. While the temperature dependence of the magnetic susceptibility and the specific heat shows only weak antiferromagnetic correlations, we find that the magnetization does not saturate up to a field of 59 T, leading to an apparent contradiction. We demonstrate that the paradox can be resolved, and all of the experimental data can be consistently described within the framework of random singlet states. We demonstrate a generic procedure to derive the exchange coupling distribution $P(J)$ from the magnetization measurements and use it to show that the experimental data are consistent with the power-law form $P(J) \sim J^{-\alpha}$ with $\alpha \approx 0.6$. Thus, we reveal that high-magnetic-field measurements can be essential to discern quantum spin-liquid candidates from disorder dominated states that do not exhibit long-range order.

DOI: 10.1103/PhysRevB.101.020406

Strong quantum fluctuations in insulating magnetic compounds can give rise to quantum spin-liquid (QSL) ground states, where the interaction-driven ordering tendencies are thwarted completely. Devoid of long-range order, QSLs lie beyond the Landau symmetry-based classification, and are characterized instead by their unconventional entanglement properties and the presence of exotic fractionalized excitations [1,2]. However, identifying the elusive QSL behavior in real materials has proven to be a formidable task [2–4]. The search for QSL candidate materials represents a major challenge of modern condensed matter physics.

Disorder is one of the major hindrances to identify QSL materials [5–7], as it can drive the formation of random singlet states (RSS) [8] or disordered stripe states [9] instead of a QSL. Importantly, this includes single-crystal samples due to intrinsic disorder [10,11]. A convenient reference point can be found in one-dimensional (1D) systems, where the quantum fluctuations are dominant [12] and the effect of disorder was clarified some time ago [13,14]. In 1D it converts the spin-liquid ground state into a RSS, where the effective exchange coupling follows a broad probability distribution that has a universal form [15] at low energies. In 2D and 3D, on the contrary, the fate of disordered spin systems is still an open question. While a random singlet state with a power-law distribution has been conjectured [16], the true ground state of such systems is still under debate and might not be universal [17–19]. In particular, enhanced suppression of QSL states by disorder has been found in model calculations [19,20]. However, mechanisms for the stabilization of QSL states by disorder have also been proposed [21]. Additionally, a strong spin-orbit coupling (SOC) is an important ingredient in many QSL candidates. While its effects on clean QSLs have been studied [1,2] and particularly emphasized for the so-called Kitaev materials [22,23], the interplay of SOC with disorder still remains to be understood. Thus, careful studies on the role of disorder and SOC in materials showing QSL-like behavior (i.e., no ordering or glassiness down to the lowest temperatures) are of the utmost importance to confirm, or rule out, the QSL state.

In this Rapid Communication, we study the magnetic and thermodynamic properties of the insulating iridate $Ba_5CuIr_3O_{12}$, which features a quasi-1D arrangement of alternating Cu^{2+} ions and Ir^{4+} trimers [25,26] (see Fig. 1). This iridate is of particular interest for the following reasons. First, previous studies [25] have shown that no magnetic ordering occurs in $Ba_5CuIr_3O_{12}$ down to 4 K despite a Curie temperature of -98 K, which suggests a possible QSL ground state. Moreover, a related compound $Ba_4NbIr_3O_{12}$ has recently been proposed to be a QSL candidate material [27]. Second, the nature of the Ir magnetic moments in this system is quite peculiar. The $5d$ Ir ions have a strong spin-orbit coupling and form face-sharing Ir^{4+} trimers, which renders the usual local $J_{\text{eff}} = 1/2$ moment picture [28,29] inapplicable due to enhanced covalency. Instead, molecular orbitals at each Ir trimer are expected to form [24,27,30]. Finally, the material

*pv184@physics.rutgers.edu
†mye@physics.rutgers.edu
‡girsh@physics.rutgers.edu

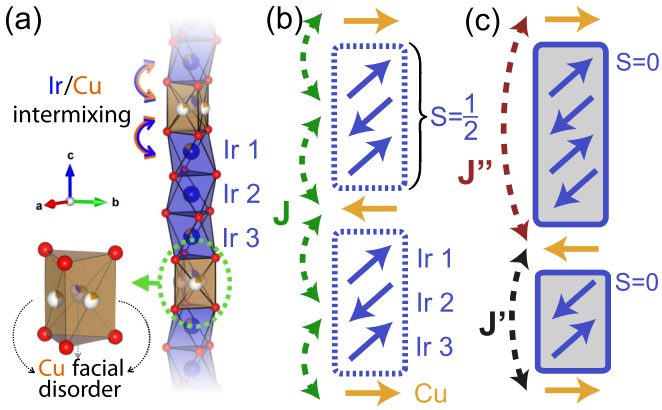

FIG. 1. The depiction of intrinsic disorder in chains of Cu and Ir in the $Ba_5CuIr_3O_{12}$ lattice structure. (a) Cu-Ir chains composed of Ir^{4+} trimers and Cu^{2+} ions (Ba ions fill the space between the chains [24]). Disorder occurs either due to Cu-Ir site mixing or due to Cu being displaced from the prism center [25,26]. (b) Spin degrees of freedom in a chain segment; here, Ir trimers form effective $J = 1/2$ moments that interact with the Cu^{2+} spins. (c) An example of disorder in the position of Cu and Ir leading to exchange disorder. Interchanging the Cu and Ir sites leads to Ir clusters forming low-spin states. The Cu spins interact with each other through perturbatively generated J' and J'', resulting in disorder in the effective magnetic exchange couplings.

contains intrinsic disorder due to site mixing between Cu and Ir, as well as Cu displacement from the prism center [25,26] [see Fig. 1(a)]. The former can lead to randomness (i.e., disorder) in the exchange couplings. A particular scenario is shown in Fig. 1(c), where interchanging Cu and Ir within a unit cell transforms two Ir trimers into a dimer and tetramer with a possible $S = 0$ ground state. As a result, the remaining Cu spins interact by means of perturbatively generated exchange couplings, that are different from the initial nonrandom value. All of the above makes $Ba_5CuIr_3O_{12}$ a well-suited candidate to explore the interplay of QSL physics with intrinsic disorder and strong spin-orbit coupling.

We have performed magnetic susceptibility, specific heat, and high-field magnetization measurements. We demonstrate that these data combined point unambiguously to $Ba_5CuIr_3O_{12}$ being in a random singlet state with a power-law distribution of exchange couplings, and thus ruling out QSL behavior. As such, we show how the high-field magnetization measurements are essential to reveal and characterize a RSS in materials that otherwise show QSL-like behavior.

Experimental techniques. We have grown single crystals of $Ba_5CuIr_3O_{12}$ using the flux method. The crystal structure and orientation were confirmed by x-ray diffraction and Laue measurements [31]. The magnetic susceptibility was measured using a superconducting quantum interference device (SQUID) magnetometer (Quantum Design) in an applied field of 0.1 T on warming after zero-field cooling to 1.8 K. The specific heat of $Ba_5CuIr_3O_{12}$ single crystals was measured using a Physical Property Measurement System (Quantum Design Dynacool). The high-field magnetization measurements have been performed at 2 K in pulsed magnetic fields up to 59 T [31] using the facilities at the Dresden High Field Magnetic Field Laboratory, described in Refs. [32–34].

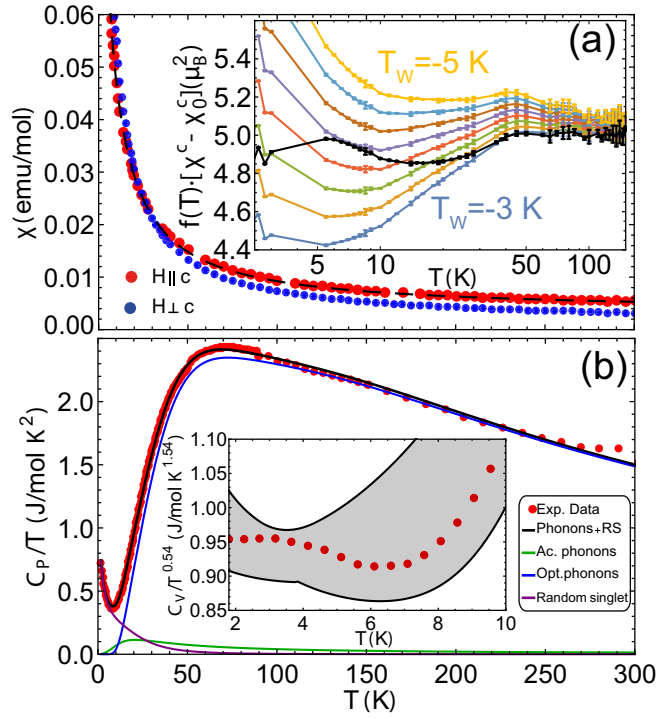

FIG. 2. Temperature (T) dependencies of the magnetic susceptibility (χ) and the specific heat (C_P). (a) The magnetic susceptibility data in red ($H \parallel c$) and blue ($H \perp c$). The black dashed line is a fit for $H \parallel c$ with the random singlet model $\chi_{RS} = \partial M_{RS}/\partial H$ [see Eq. (1)]. Inset: $(\chi^c - \chi_0^c)$ multiplied by a function $f(T)$. For the colored points we take $f(T) = 3(T - T_W)$ for several values of T_W between -3 and -5 K, for $H \parallel c$, demonstrating the nonlinearity of the low-temperature dependence. Black points are the RSS contribution $f(T) = \chi_{RS}(T)/\mu_{eff}^2$. Lines are guides to the eye. At high temperatures all curves converge to μ_{eff}^2. (b) Specific heat divided by temperature. The black line is a fit to the combination of the random singlet model in Eq. (2) and a simplified model for phonons (see text). Inset: The specific heat divided by $T^{0.54}$; the gray band shows the confidence interval of the fit.

Magnetic susceptibility. In Fig. 2(a) we show the temperature dependence of the magnetic susceptibility for fields along the c axis, $\chi^c(T)$, or in the a-b plane, $\chi^{ab}(T)$. Both $\chi^c(T)$ and $\chi^{ab}(T)$ show a featureless monotonic increase towards low temperatures and a weak anisotropy [31]. At high temperatures, a constant contribution χ_0 in addition to the Curie behavior can be identified, which is attributed to Van Vleck paramagnetism. The effective moment that is obtained from the Curie law fit is $\mu_{eff} = 2.2\mu_B$, which is close to the value that is expected from one Cu^{2+} moment ($\mu_{eff}^{Cu} = 1.9\mu_B$) and one Ir trimer ($\mu_{eff}^{Ir\text{-}tr} = 0.8\mu_B$) [27] that yield $\sqrt{(\mu_{eff}^{Cu})^2 + (\mu_{eff}^{Ir\text{-}tr})^2} \approx 2.06\mu_B$.

In an earlier study on polycrystalline samples [25], the susceptibility was analyzed using a modified Curie-Weiss model for temperatures between 150 and 300 K. Using $\chi(T) = C/(T - T_W) + \chi_0$ resulted in a large negative Weiss temperature $T_W = -98$ K. Analyzing our data, we have come to the conclusion that the Curie-Weiss model does not provide an adequate description. First, if the analysis is restricted to high temperatures, large uncertainties in the value of T_W result

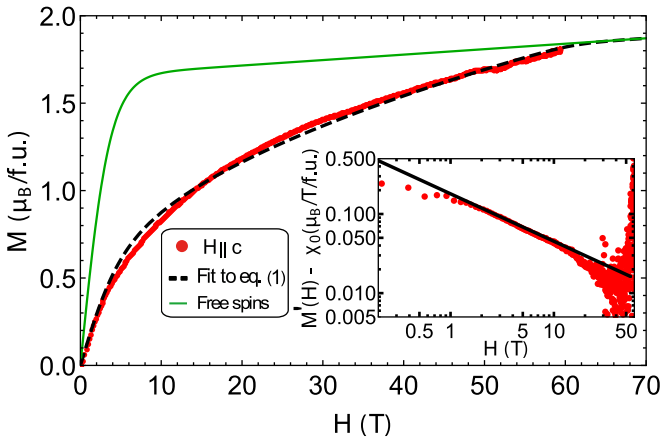

FIG. 3. The magnetic field dependence of the magnetization at $T = 2$ K for the field along the c-axis direction. The weak kink near 50 T results from the noise of the equipment. The black dashed line is a fit with the random singlet model [Eq. (1)] using the parameters given in Table I. The green line represents the magnetization of an $S = 1/2$ paramagnet. The Van Vleck contribution $H\chi_0$ has been added to both. Inset: Log-log plot of $dM(H)/dH - \chi_0$ for the field along the c axis, and the black line is a power-law fit $0.18H^{-0.6}$. Data for $H \parallel ab$ are not shown due to calibration issues [31].

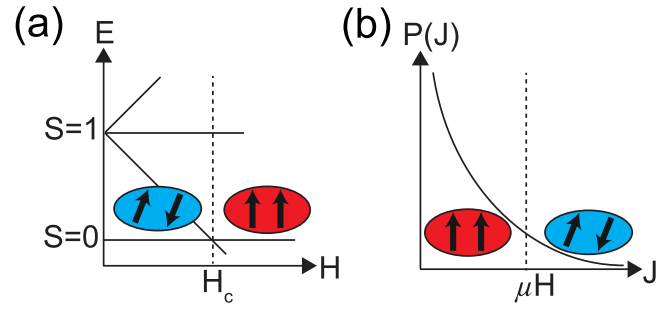

FIG. 4. (a) The energy levels and the ground state of an isolated singlet. The triplet ($S = 1$) of excited states at $H = 0$ is split in the field, and a change of the ground state occurs at $H_c(J)$, from singlet ($S = 0$) to fully polarized ($S = 1$). (b) The random singlet distribution in a magnetic field. Singlets with $J < \mu H$ are broken by the field and are fully polarized, while the ones with $J > \mu H$ remain in the singlet state, leading to a nonsaturating magnetization.

[31]. Second, at low temperatures $(\chi - \chi_0)^{-1}$ is not linear as would have been expected from the Curie-Weiss form. We demonstrate this in the inset of Fig. 2(a) by showing $(T - T_W)(\chi^c - \chi_0^c)^{-1}$ for a range of T_W from -3 to -5 K. Additionally, one can see that larger or smaller values of T_W would lead to even larger deviations, suggesting weak antiferromagnetic (AFM) correlations.

This is further corroborated by noting that even in the absence of order, anomalies in $\chi(T)$ are expected to arise at a temperature corresponding to the interaction scale in 1D antiferromagnetic chains [35,36], spin glasses [37,38], and spin liquids with AFM interactions [39]. The absence of such features in Fig. 2(a) implies that the relevant interaction scale is lower than 2 K. We have also confirmed the absence of glassy behavior above 2 K by performing low-field (100-Oe) field-cooled/zero-field-cooled (FC/ZFC) susceptibility measurements [31].

Specific heat. In Fig. 2(b) we show the temperature dependence of the specific heat $C_P(T)$. The high-temperature behavior of $C_P(T)/T$ is dominated by the phonon contribution, which freezes out as the temperature is lowered. Thus, the dramatic upturn that is observed below $\sim$10 K must be of magnetic origin. As no Schottky-like peak is observed down to 2 K, the energy scale associated with these magnetic excitations should be below 2 K. This is consistent with the weak AFM correlations conjectured above on the basis of the $\chi(T)$ measurements.

High-field magnetization. Surprisingly, the field dependence of the magnetization $M(H)$ is in stark contrast with the expectation from weak AFM correlations (see Fig. 3). Namely, $M(H)$ shows a monotonic increase without saturation up to the highest fields measured, 59 T. To illustrate this, we show in Fig. 3 (green line) the $M(H)$ that is expected for a system of two free $S = 1/2$ spins per unit cell, with an effective moment $\mu_{\rm eff}/\sqrt{2}$ each, and taking the Van Vleck contribution $M_{\rm VV} = \chi_0 H$ into account. One can see that within such a model the magnetization would have saturated well below 59 T, implying that the magnetic interactions in $Ba_5CuIr_3O_{12}$ must be rather strong. One can estimate the scale of the interactions assuming the $S = 1/2$ moments mentioned above to form singlets with an isotropic exchange energy J. The magnetization would then saturate when the Zeeman energy $E_Z = HgS = H\mu_{\rm eff}\sqrt{S/(S+1)}$ for the triplet excitation reaches J (see Fig. 4). As the saturation field is at least larger than 59 T, we estimate $J \gtrsim 70$ K. On the contrary, the energy scales we have derived above from the susceptibility and specific heat measurements are below 2 K. In addition, in systems with AFM interactions the shape of the magnetization curve as a function of H is usually convex [35,40–42] at low temperatures, while the $M(H)$ curve shown in Fig. 3 is clearly concave, further making the interpretation of the high-field magnetization in terms of a strong AFM exchange interaction problematic.

Random singlet state. We will now show that the conflict between the energy scales that we have seen in low- and high-field measurements can be resolved by assuming a *distribution* of energy scales in the system in the framework of a RSS. The exchange disorder driving the RSS can result from the intrinsic positional disorder between Cu and Ir observed in x-ray [25] and neutron scattering [26] experiments, as discussed above and illustrated for a particular scenario in Fig. 1(c). Other possible scenarios would involve nonstoichometric compositions within one unit cell, e.g., simply substituting one Cu for Ir.

Given the small magnetic anisotropy observed in $\chi(T)$ [see Fig. 2(a)], we consider an ensemble of singlets formed by two effective $S = 1/2$ moments with a total magnetic moment μ, and with an isotropic random exchange coupling J that is drawn from the distribution $P(J)$. The magnetization of the whole system is then an average of the magnetization of each isolated singlet, and is given by

$$M_{\rm RS}(H) = \int_0^\infty dJ P(J) \frac{2\mu \sinh(\beta\mu H)}{2\cosh(\beta\mu H) + 1 + e^{\beta J}}, \quad (1)$$

TABLE I. The power-law exponents α and the cutoff scale J_0 are obtained by fitting the magnetic susceptibility, magnetization, and heat capacity data with the corresponding confidence intervals. The resulting fits are plotted in Figs. 2 and 3.

Measured quantity	α	J_0 (K)
$\chi^c(T)$	0.62 ± 0.02	36 ± 1
$\chi^{ab}(T)$	0.66 ± 0.01	16.3 ± 0.4
$M_c(H)$	0.64 ± 0.01	67.8 ± 0.4
$C_p(T)$	0.55 ± 0.05	95 ± 5

where $\beta = 1/(k_B T)$. We account for the Van Vleck contribution as before for free spins, i.e., $M(H) = M_{\rm RS}(H) + H\chi_0$. Qualitatively, Eq. (1) allows a coexistence of almost free spins that can yield a diverging susceptibility towards $T = 0$ and strongly bound singlets from the high-J tail of the distribution that require the applied field to be above a threshold value for the magnetization to saturate (see Fig. 4). Importantly, in the limit $T \ll \mu H$ one obtains from Eq. (1) that $M'(H) \approx \chi_0 + \mu^2 P(\mu H)$, allowing one to extract the functional form of the distribution $P(J)$ directly from the experimental data. We find that $P(\mu H)$ follows the power-law form $P(\mu H) \sim H^{-0.6}$ for fields between 1 and 15 T (see Fig. 3, inset).

Let us now discuss the specific heat. Similarly to the magnetization, the contribution of the RSS is an average over specific heats of individual singlets,

$$C_{\rm RS}(T) = k_B \int_0^\infty dJ P(J) \frac{J^2}{T^2} \frac{3e^{-J/T}}{(1+3e^{-J/T})^2}. \qquad (2)$$

For $P(J) \sim J^{-\alpha}$ it follows that at low temperatures $C_{\rm RS} \sim T^{(1-\alpha)}$. Indeed, we find that below about 4 K, $C_P \sim T^{0.54}$ [see Fig. 2(b), inset] that suggests the power-law exponent to be 0.46. The discrepancy of this value with the one obtained from the high-field magnetization can be attributed to $P(J)$ having a slightly different form for low and moderate J, as the specific heat (2) is most sensitive to $P(J)$ below $J \approx 4$ K, while the power law in the magnetization is extracted for larger values of J. Nonetheless, the discrepancy between the power-law exponents is not too large.

Hence, we have attempted to fit the data from each measurement with a single form of $P(J) = \theta(J_0 - J)J^{-\alpha}$, where a cutoff scale J_0 has been introduced to ensure proper normalization. The results of the fits are given in Table I. The parameter μ in Eq. (1) is related to $\mu_{\rm eff}$ at high temperatures as $\mu = \sqrt{2/3}\,\mu_{\rm eff}$. Additionally, to describe the specific heat at all temperatures, we have modeled the phonon contribution of specific heat with a combination of Debye and Einstein phonons [31], i.e., $C_P(T) = C_{\rm RS}(T) + C_{\rm phon}(T)$.

The resulting fits to the data are excellent, as shown in Figs. 2 and 3. Importantly, the qualitative features of all three measurements are well captured: The susceptibility increasing nonlinearly at low T [see the inset of Fig. 2(a)], the upturn in the specific heat at low T where $C_{\rm RS}$ dominates, and the nonsaturating concave high-field magnetization. Moreover, the resulting power-law exponents obtained from fits across different experiments agree well with each other (see Table I). The cutoff scale J_0, on the contrary, shows significant variations. This can be partially attributed to the deviations of $P(J)$ from the power-law form at the lowest and highest values of J (as is seen in Fig. 3), as different quantities are most sensitive to different ranges of J values. Additionally, it can be shown that this parameter depends on the way the cutoff is implemented—e.g., implementation of a soft cutoff affects the value of J_0 [31]. Thus, we argue that the variations of J_0 reflect the approximate character of the form of $P(J)$ we use, which is nonetheless sufficient for the qualitative description of the data.

As has been mentioned above, the distribution parameters may vary between the low- and intermediate-energy scales. The agreement of the power-law exponents in Table I with the one obtained from magnetization between 1 and 15 T suggests that these values do not concern the distribution at very low energies. Instead, we have established the presence of random singlet excitations with a unique power-law form in the intermediate-energy range.

Summary. By combining low- and high-magnetic-field measurements we have established that $Ba_5CuIr_3O_{12}$ at low temperatures is well described as a random singlet state. We have shown that a nonsaturating high-field magnetization allows one to rule out a QSL scenario and quantitatively extract the exchange coupling distribution of the random singlet state $P(J) \sim J^{-0.6}$ at intermediate energies. We find the extracted power-law distribution is consistent across the magnetization, susceptibility, and specific heat measurements. Thus, we establish that a combination of high-field measurements with more conventional techniques allows one to study the role of disorder in QSL candidate materials as well as characterize strongly disordered ground states.

Acknowledgments. Crystal growth was supported by the National Research Foundation of Korea, Ministry of Science and ICT (No. 2016K1A4A4A01922028), and magnetic measurement was supported by the NSF under Grant No. DMR-1629059. We acknowledge the support of HLD at HZDR, member of the European Magnetic Field Laboratory (EMFL). The work was supported by the DFG through SFB 1143. The spectroscopic characterization at Rutgers (M.Y. and G.B.) was supported by NSF Grant No. DMR-1709161. J.H.P. was supported by Grant No. 2018058 from the United States-Israel Binational Science Foundation (BSF), Jerusalem, Israel and acknowledges the Aspen Center for Physics where some of this work was performed, which is supported by National Science Foundation Grant No. PHY-1607611. P.A.V. acknowledges the Postdoctoral Fellowship support from the Rutgers University Center for Materials Theory.

[1] L. Savary and L. Balents, Quantum spin liquids: A review, Rep. Prog. Phys. **80**, 016502 (2016).

[2] Y. Zhou, K. Kanoda, and T.-K. Ng, Quantum spin liquid states, Rev. Mod. Phys. **89**, 025003 (2017).

[3] M. R. Norman, *Colloquium:* Herbertsmithite and the search for the quantum spin liquid, Rev. Mod. Phys. **88**, 041002 (2016).

[4] J. Wen, S.-L. Yu, S. Li, W. Yu, and J.-X. Li, Experimental identification of quantum spin liquids, npj Quantum Mater. **4**, 12 (2019).

[5] J. S. Helton, K. Matan, M. P. Shores, E. A. Nytko, B. M. Bartlett, Y. Qiu, D. G. Nocera, and Y. S. Lee, Dynamic Scaling in the Susceptibility of the Spin-$\frac{1}{2}$ Kagome Lattice Antiferromagnet Herbertsmithite, Phys. Rev. Lett. **104**, 147201 (2010).

[6] I. Kimchi, J. P. Sheckelton, T. M. McQueen, and P. A. Lee, Scaling and data collapse from local moments in frustrated disordered quantum spin systems, Nat. Commun. **9**, 4367 (2018).

[7] Y. S. Choi, C. H. Lee, S. Lee, S. Yoon, W.-J. Lee, J. Park, A. Ali, Y. Singh, J.-C. Orain, G. Kim, J.-S. Rhyee, W.-T. Chen, F. Chou, and K.-Y. Choi, Exotic Low-Energy Excitations Emergent in the Random Kitaev Magnet Cu_2IrO_3, Phys. Rev. Lett. **122**, 167202 (2019).

[8] I. Kimchi, A. Nahum, and T. Senthil, Valence Bonds in Random Quantum Magnets: Theory and Application to $YbMgGaO_4$, Phys. Rev. X **8**, 031028 (2018).

[9] Z. Zhu, P. A. Maksimov, S. R. White, and A. L. Chernyshev, Disorder-Induced Mimicry of a Spin Liquid in $YbMgGaO_4$, Phys. Rev. Lett. **119**, 157201 (2017).

[10] Y. Li, G. Chen, W. Tong, L. Pi, J. Liu, Z. Yang, X. Wang, and Q. Zhang, Rare-Earth Triangular Lattice Spin Liquid: A Single-Crystal Study of $YbMgGaO_4$, Phys. Rev. Lett. **115**, 167203 (2015).

[11] Y. Li, S. Bachus, B. Liu, I. Radelytskyi, A. Bertin, A. Schneidewind, Y. Tokiwa, A. A. Tsirlin, and P. Gegenwart, Rearrangement of Uncorrelated Valence Bonds Evidenced by Low-Energy Spin Excitations in $YbMgGaO_4$, Phys. Rev. Lett. **122**, 137201 (2019).

[12] T. Giamarchi, *Quantum Physics in One Dimension* (Oxford University Press, New York, 2004).

[13] S.-k. Ma, C. Dasgupta, and C.-k. Hu, Random Antiferromagnetic Chain, Phys. Rev. Lett. **43**, 1434 (1979).

[14] J. E. Hirsch and J. V. José, Singular thermodynamic properties in random magnetic chains, Phys. Rev. B **22**, 5339 (1980).

[15] D. S. Fisher, Random antiferromagnetic quantum spin chains, Phys. Rev. B **50**, 3799 (1994).

[16] R. N. Bhatt and P. A. Lee, Scaling Studies of Highly Disordered Spin-1/2 Antiferromagnetic Systems, Phys. Rev. Lett. **48**, 344 (1982).

[17] O. Motrunich, S.-C. Mau, D. A. Huse, and D. S. Fisher, Infinite-randomness quantum Ising critical fixed points, Phys. Rev. B **61**, 1160 (2000).

[18] Y.-C. Lin, R. Mélin, H. Rieger, and F. Iglói, Low-energy fixed points of random Heisenberg models, Phys. Rev. B **68**, 024424 (2003).

[19] H. Kawamura, K. Watanabe, and T. Shimokawa, Quantum spin-liquid behavior in the spin-1/2 random-bond Heisenberg antiferromagnet on the kagome lattice, J. Phys. Soc. Jpn. **83**, 103704 (2014).

[20] K. Uematsu and H. Kawamura, Randomness-induced quantum spin liquid behavior in the $s = \frac{1}{2}$ random J_1-J_2 Heisenberg antiferromagnet on the square lattice, Phys. Rev. B **98**, 134427 (2018).

[21] H.-Q. Wu, S.-S. Gong, and D. N. Sheng, Randomness-induced spin-liquid-like phase in the spin-$\frac{1}{2}$ J_1-J_2 triangular Heisenberg model, Phys. Rev. B **99**, 085141 (2019).

[22] J. Knolle and R. Moessner, A field guide to spin liquids, Annu. Rev. Condens. Matter Phys. **10**, 451 (2019).

[23] H. Takagi, T. Takayama, G. Jackeli, G. Khaliullin, and S. E. Nagler, Concept and realization of Kitaev quantum spin liquids, Nat. Rev. Phys. **1**, 264 (2019).

[24] M. Ye, H.-S. Kim, J.-W. Kim, C.-J. Won, K. Haule, D. Vanderbilt, S.-W. Cheong, and G. Blumberg, Covalency-driven collapse of strong spin-orbit coupling in face-sharing iridium octahedra, Phys. Rev. B **98**, 201105(R) (2018).

[25] G. R. Blake, J. Sloan, J. F. Vente, and P. D. Battle, Prediction and verification of the structural chemistry of new one-dimensional barium/copper/iridium oxides, Chem. Mater. **10**, 3536 (1998).

[26] G. R. Blake, P. D. Battle, J. Sloan, J. F. Vente, J. Darriet, and F. Weill, Neutron diffraction study of the structures of $Ba_5CuIr_3O_{12}$ and $Ba_{16}Cu_3Ir_{10}O_{39}$, Chem. Mater. **11**, 1551 (1999).

[27] L. T. Nguyen and R. J. Cava, Trimer-based spin liquid candidate $Ba_4NbIr_3O_{12}$, Phys. Rev. Materials **3**, 014412 (2019).

[28] B. J. Kim, H. Jin, S. J. Moon, J.-Y. Kim, B.-G. Park, C. S. Leem, J. Yu, T. W. Noh, C. Kim, S.-J. Oh, J.-H. Park, V. Durairaj, G. Cao, and E. Rotenberg, Novel $J_{\rm eff} = 1/2$ Mott State Induced by Relativistic Spin-Orbit Coupling in Sr_2IrO_4, Phys. Rev. Lett. **101**, 076402 (2008).

[29] B. J. Kim, H. Ohsumi, T. Komesu, S. Sakai, T. Morita, H. Takagi, and T. Arima, Phase-sensitive observation of a spin-orbital Mott state in Sr_2IrO_4, Science **323**, 1329 (2009).

[30] S. V. Streltsov and D. I. Khomskii, Orbital physics in transition metal compounds: New trends, Phys.-Usp. **60**, 1121 (2017).

[31] See Supplemental Material at http://link.aps.org/supplemental/10.1103/PhysRevB.101.020406 for the details of the crystal growth procedure, calibration of the high-field measurements, random singlet model and the fitting procedure, as well as magnetic anisotropy and zero-field-cooled measurements, which includes Refs. [24–27,43–47].

[32] S. Zherlitsyn, A. D. Bianchi, T. Herrmannsdoerfer, F. Pobell, Y. Skourski, A. Sytcheva, S. Zvyagin, and J. Wosnitza, Coil design for non-destructive pulsed-field magnets targeting 100 T, IEEE Trans. Appl. Supercond. **16**, 1660 (2006).

[33] J. Wosnitza, A. D. Bianchi, J. Freudenberger, J. Haase, T. Herrmannsdorfer, N. Kozlova, L. Schultz, Y. Skourski, S. Zherlitsyn, and S. A. Zvyagin, Dresden pulsed magnetic field facility, J. Magn. Magn. Mater. **310**, 2728 (2007).

[34] Y. Skourski, M. D. Kuz'min, K. P. Skokov, A. V. Andreev, and J. Wosnitza, High-field magnetization of Ho_2Fe_{17}, Phys. Rev. B **83**, 214420 (2011).

[35] J. C. Bonner and M. E. Fisher, Linear magnetic chains with anisotropic coupling, Phys. Rev. **135**, A640 (1964).

[36] S. Eggert, I. Affleck, and M. Takahashi, Susceptibility of the Spin 1/2 Heisenberg Antiferromagnetic Chain, Phys. Rev. Lett. **73**, 332 (1994).

[37] K. Binder and A. P. Young, Spin glasses: Experimental facts, theoretical concepts, and open questions, Rev. Mod. Phys. **58**, 801 (1986).

[38] J. A. Mydosh, Spin glasses: Redux: An updated experimental/materials survey, Rep. Prog. Phys. **78**, 052501 (2015).

[39] J. Yoshitake, J. Nasu, and Y. Motome, Fractional Spin Fluctuations as a Precursor of Quantum Spin Liquids: Majorana

Dynamical Mean-Field Study for the Kitaev Model, Phys. Rev. Lett. **117**, 157203 (2016).

[40] R. B. Griffiths, Magnetization curve at zero temperature for the antiferromagnetic Heisenberg linear chain, Phys. Rev. **133**, A768 (1964).

[41] V. A. Kashurnikov, N. V. Prokof'ev, B. V. Svistunov, and M. Troyer, Quantum spin chains in a magnetic field, Phys. Rev. B **59**, 1162 (1999).

[42] T. Shimokawa, K. Watanabe, and H. Kawamura, Static and dynamical spin correlations of the $s = \frac{1}{2}$ random-bond antiferromagnetic Heisenberg model on the triangular and kagome lattices, Phys. Rev. B **92**, 134407 (2015).

[43] G. Khaliullin, Orbital order and fluctuations in Mott insulators, Prog. Theor. Phys. Suppl. **160**, 155 (2005).

[44] J. G. Rau, E. K.-H. Lee, and H.-Y. Kee, Spin-orbit physics giving rise to novel phases in correlated systems: Iridates and related materials, Annu. Rev. Condens. Matter Phys. **7**, 195 (2016).

[45] J. Bertinshaw, Y. K. Kim, G. Khaliullin, and B. J. Kim, Square lattice iridates, Annu. Rev. Condens. Matter Phys. **10**, 315 (2019).

[46] K. A. Modic, T. E. Smidt, I. Kimchi, N. P. Breznay, A. Biffin, S. Choi, R. D. Johnson, R. Coldea, P. Watkins-Curry, G. T. McCandless, J. Y. Chan, F. Gandara, Z. Islam, A. Vishwanath, A. Shekhter, R. D. McDonald, and J. G. Analytis, Realization of a three-dimensional spin-anisotropic harmonic honeycomb iridate, Nat. Commun. **5**, 4203 (2014).

[47] H. Ishizuka, Temperature-dependent magnetic anisotropy from pseudo-dipolar interactions, Phys. Rev. B **95**, 184413 (2017).